Glial Depolarization Evokes a Larger Potassium Accumulation Around Oligodendrocytes Than Around Astrocytes in Gray Matter of Rat Spinal Cord Slices

Alexandr Chvátal,[1,2]* **Miroslava Anděrová,**[1,2] **Drahomír Žiak,**[1] **and Eva Syková**[1,2]
[1]Department of Neuroscience, Institute of Experimental Medicine, Academy of Sciences of the Czech Republic, Prague, Czech Republic
[2]Department of Neuroscience, Second Medical Faculty, Charles University, Prague, Czech Republic

The cell membrane of astrocytes and oligodendrocytes is almost exclusively permeable for K^+. Depolarizing and hyperpolarizing voltage steps produce in oligodendrocytes, but not in astrocytes, decaying passive currents followed by large tail currents (I_{tail}) after the offset of a voltage jump. The aim of the present study was to characterize the properties of I_{tail} in astrocytes, oligodendrocytes, and their respective precursors in the gray matter of spinal cord slices. Studies were carried out on 5- to 11-day-old rats, using the whole-cell patch clamp technique. The reversal potential (V_{rev}) of I_{tail} evoked by membrane depolarization was significantly more positive in oligodendrocytes (-31.7 ± 2.58 mV, n = 53) than in astrocytes (-57.9 ± 2.43 mV, n = 21), oligodendrocyte precursors (-41.2 ± 3.44 mV, n = 36), or astrocyte precursors (-52.1 ± 1.32 mV, n = 43). Analysis of the I_{tail} (using a variable amplitude and duration of the de- and hyperpolarizing prepulses as well as an analysis of the time constant of the membrane currents during voltage steps) showed that the I_{tail} in oligodendrocytes arise from a larger shift of K^+ across their membrane than in other cell types. As calculated from the Nernst equation, changes in V_{rev} revealed significantly larger accumulation of the extracellular K^+ concentration ($[K^+]_e$) around oligodendrocytes than around astrocytes. The application of 50 mM K^+ or hypotonic solution, used to study the effect of cell swelling on the changes in $[K^+]_e$ evoked by a depolarizing prepulse, produced in astrocytes an increase in $[K^+]_e$ of 201% and 239%, respectively. In oligodendrocytes, such increases (22% and 29%) were not found. We conclude that K^+ tail currents, evoked by a larger accumulation of K^+ in the vicinity of the oligodendrocyte membrane, could result from a smaller extracellular space (ECS) volume around oligodendrocytes than around astrocytes. Thus, in addition to the clearance of K^+ from the ECS performed by astrocytes, the presence of the K^+ tail currents in oligodendrocytes indicates that they might also contribute to efficient K^+ homeostasis. J. Neurosci. Res. 56:493–505, 1999.
© 1999 Wiley-Liss, Inc.

Key words: K^+ tail currents; extracellular space; astrocytes; oligodendrocytes; development

INTRODUCTION

Glial cells, similar to neurons, express a number of voltage-gated K^+ channels, including outward delayed rectifier, A-type, and inward rectifier channels (for review, see Barres et al., 1990; Duffy et al., 1995). However, glial cells posses greater selective potassium permeability, which results in a more negative resting membrane potential, than seen in neurons. This selective potassium permeability in glial cells allows them to buffer extracellular K^+ changes resulting from neuronal activity and thus to maintain K^+ homeostasis in the brain cell microenvironment (Kuffler et al., 1966; for reviews see Syková, 1983; Walz, 1989; Syková, 1992).

The electrophysiological properties of identified glial cells in situ have been studied by means of the whole-cell patch-clamp technique in brain slices prepared from different regions of the CNS, including hippocampus (Steinhäuser et al., 1992), corpus callosum (Berger et

al., 1991; Chvátal et al., 1997), and spinal cord (Chvátal et al., 1995; Pastor et al., 1995; Žiak et al., 1998). These studies revealed that astrocyte and oligodendrocyte precursor cells are characterized by the presence of voltage-gated K^+ channels, while mature astrocytes and oligodendrocytes are characterized by large passive currents during membrane depolarization or hyperpolarization. In contrast to astrocytes, passive currents in oligodendrocytes decay during the voltage step, and tail currents are observed after the offset of the voltage jump. The hypothesis that current decay in oligodendrocytes is caused by a shift of K^+ across the cell membrane was postulated by Berger et al. (1991).

In our previous study on glial cells in the rat corpus callosum (Chvátal et al., 1997), we have found that the reversal potential of tail currents was shifted to more positive values in mature oligodendrocytes at postnatal day 20 (P20) than in oligodendrocyte precursors at P10, even when comparable outward currents were evoked during the depolarizing voltage step. One possible explanation for this observation is that K^+ is extruded into a more compact extracellular space (ECS) at P20 than at P10 and thus accumulates to a higher concentration outside the glial cell membrane. It was found in the same study, as well as in the study of Voříšek and Syková (1997) using the real-time iontophoretic method of diffusion analysis, that the ECS volume decreased from 36% of total tissue volume at P9–10 to 25% at P20–21. Therefore, it was concluded that in myelinated rat corpus callosum, as a result of the reduced extracellular volume, membrane fluxes produce larger changes in extracellular K^+ concentration than before myelination.

In the present study, we analyzed the tail currents of electrophysiologically and morphologically identified astrocytes, oligodendrocytes, and glial precursor cells in gray matter of rat spinal cord slices during postnatal development from P5 to P11. We investigated the origin and properties of the tail currents and their relation to the changes of the extracellular space volume.

MATERIALS AND METHODS

Preparation of Spinal Cord Slices and Patch-Clamp Setup

Spinal cord slices were prepared as described previously (Chvátal et al., 1995). In brief, young rats were sacrificed under ether anesthesia at postnatal days 5 to 11 (P5–11) by decapitation. The spinal cords were quickly dissected and washed in artificial cerebrospinal fluid (ACF) at 8–10°C. A 4- to 5-mm-long segment of the lumbar cord was embedded in 1.7% agar at 37°C (Purified Agar, Oxoid Ltd., U.K.). Transverse 200-μm-thick slices were made using a vibroslice (752M, Campden Instruments, U.K.). Slices were placed in a chamber mounted on the stage of a fluorescence microscope (Axioskop FX, Carl Zeiss, Germany) and fixed using a U-shaped platinum wire with a grid of nylon threads (Edwards et al., 1989). The chamber was continuously perfused with oxygenated ACF. All experiments were carried out at room temperature (~22°C). Cell somata in the spinal cord slice were approached by the patch electrode using an INFRAPATCH system (Luigs & Neumann, Ratingen, Germany). One cell per slice was examined; individual slices were used for recording for no longer than 60 minutes.

The cells in the slice and the recording electrode were imaged with an infrared-sensitive video camera (C2400-03, Hamamatsu Photonics, Hamamatsu City, Japan) and displayed on a standard TV/video monitor. Selected cells with a membrane potential more negative than −60 mV had a clear, dark membrane surface and were located 5–10 μm below the slice surface. Membrane currents were measured with the patch-clamp technique in the whole-cell recording configuration (Hamill et al., 1981). Current signals were amplified with an EPC-9 amplifier (HEKA elektronik, Lambrecht/Pfalz, Germany), filtered at 3 kHz and sampled at 5 kHz by an interface connected to an AT-compatible computer system, which also served as a stimulus generator.

Solutions and Electrodes

The ACF contained (in mM): NaCl 117.0, KCl 3.0, $CaCl_2$ 1.5, $MgCl_2$ 1.3, Na_2HPO_4 1.25, $NaHCO_3$ 35.0, D-Glucose 10.0, osmolality 300 mmol/kg. The solution was continuously gassed with a mixture of 95% O_2 and 5% CO_2 (Linde Technoplyn, Prague, Czech Republic) to maintain a final pH of 7.4. ACF containing 50 mM K^+ had a reciprocally reduced Na^+ concentration. Hypoosmotic ACF (200 mmol/kg) had a reduced concentration of NaCl. Osmolality was measured using a vapor pressure osmometer (Vapro 5520, Wescor Inc., Logan, UT). The perfusion rate of the ACF in the recording chamber (~2 ml volume) was 5 ml/min.

Recording pipettes (4-6 MΩ) were pulled from borosilicate capillaries (Kavalier, Otvovice, Czech Republic) using a Brown-Flaming micropipette puller (P-97, Sutter Instruments Company, Novato, CA). The internal pipette solution had the following composition (in mM): KCl 130.0, $CaCl_2$ 0.5, $MgCl_2$ 2.0, EGTA 5.0, HEPES 10.0. The pH was adjusted with KOH to 7.2. The pipette always contained 1 mg/ml Lucifer Yellow Dilithium salt (Sigma, St. Louis, MO).

During electrophysiological measurements, cells were filled with Lucifer Yellow by dialyzing the cytoplasm with the patch pipette solution. After recording, the morphology of Lucifer Yellow-filled cells was studied in an unfixed spinal cord slice using a fluorescence microscope equipped with a fluorescein isothiocyanate filter combination (band pass 450–490 nm, mirror 510 nm, long pass 520 nm).
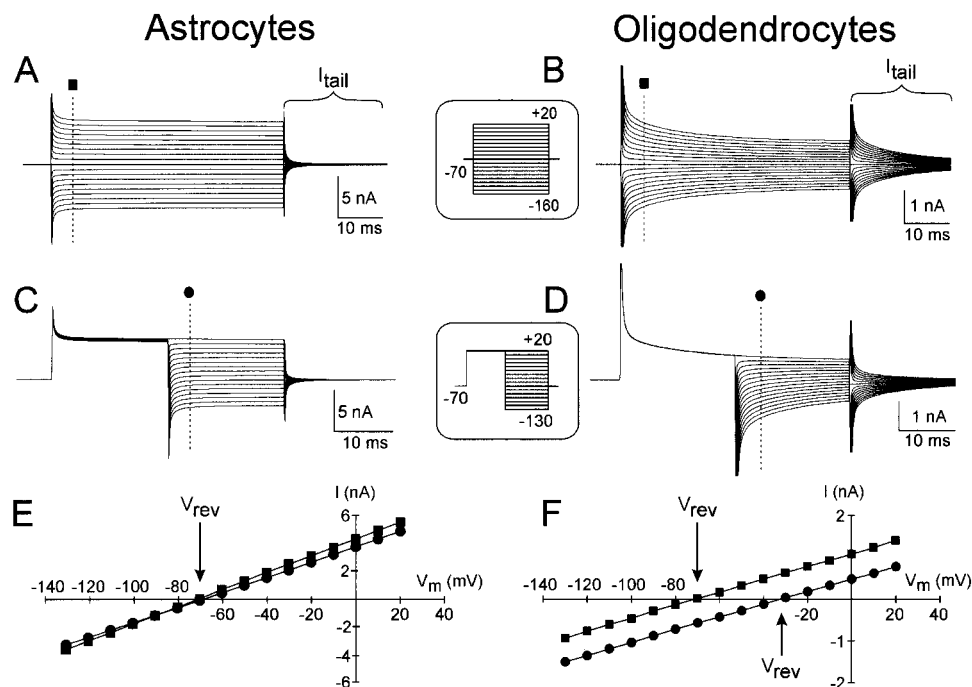
Fig. 1. Membrane properties and tail current analysis in astrocytes (A, C, E) and oligodendrocytes (B, D, F). **A, B:** Membrane currents were recorded in response to voltage steps from a holding potential of −70 mV. To activate currents, the membrane was clamped for 50 ms to increasing de- and hyperpolarizing potentials (pattern of voltage commands in **inset**) ranging from −160 to +20 mV, at 10-mV increments. The corresponding current traces are superimposed. **C, D:** For the tail current analysis, the membranes of astrocytes and oligodendrocytes were clamped from a holding potential of −70 mV to +20 mV for 20 ms. After this prepulse, the membrane was clamped for 20 ms to increasing de- and hyperpolarizing potentials (pattern of voltage commands in **inset**) ranging from −130 mV to +20 mV, at 10-mV increments. **E, F:** From traces as shown in A–D, currents (I) were measured 5 ms after the onset of the de- and hyperpolarizing pulses (dashed lines) and plotted as a function of the membrane potential (V_m). The reversal potentials (V_{rev}) are indicated in the graphs by the arrows. In the oligodendrocyte, in contrast to the astrocyte, the depolarizing prepulse shifted the reversal potential from −70 mV to −31 mV.

Statistical Analysis

Results are expressed as the mean ± S.E.M. Linear regression was used to find the line that best predicts the reversal potential of the tail currents as a function of the age of the animal. The *P* value was used to determine whether the slope of the linear regression was significantly different from zero. Values of $P < 0.05$ were considered significant.

RESULTS

Electrophysiological and Morphological Identification of Glial Cells

Experiments were performed on glial cells in the gray matter of rat spinal cord slices from 5- to 11-day-old animals (P5–11). Membrane currents were activated by clamping the glial cell membrane from the holding potential of −70 mV to values ranging from −160 mV to +20 mV. The current patterns after de- and hyperpolarizing pulses and the morphology of glial cells filled with the fluorescent dye Lucifer Yellow distinguished among astrocytes, oligodendrocytes, and their respective precursors. Glial cells were classified on the basis of our previous electrophysiological, morphological, and immunohistochemical analyses of glial cells in rat spinal cord slices (Chvátal et al., 1995; Pastor et al., 1995).

Electrophysiologically, astrocytes were characterized by large, symmetrical, nondecaying K$^+$-selective currents during the voltage jump (Fig. 1A), oligodendrocytes by symmetrical passive but decaying K$^+$ currents (Fig. 1B). After the offset of the depolarizing or hyperpolarizing voltage step, large symmetrical inward and outward tail currents (I$_{tail}$) appeared in oligodendrocytes. These currents were not observed in astrocytes. In oligodendrocytes, I$_{tail}$ decayed with a similar time constant as the currents evoked by the voltage step. Astrocyte precursor cells were characterized by the presence of voltage-activated channels, namely inward rectifying, delayed outward rectifying, and A-type K$^+$ currents, and Na$^+$ currents (Fig. 2A). Oligodendrocyte precursor cells
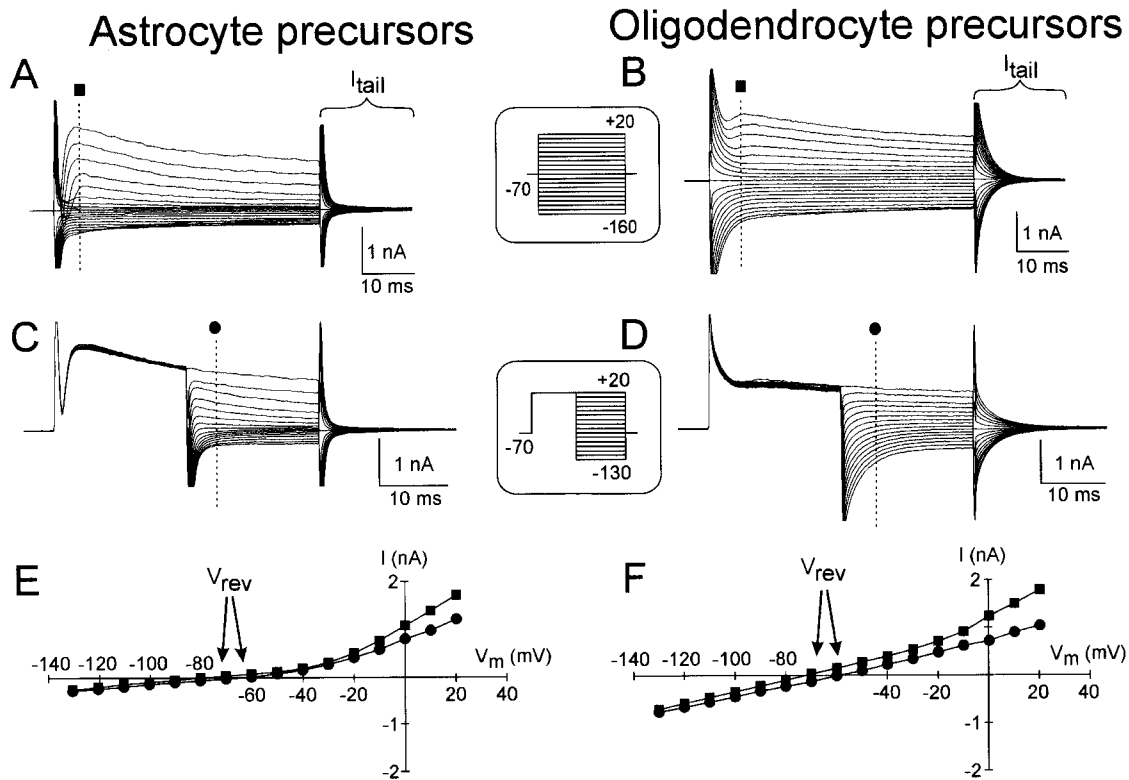
Fig. 2. Membrane properties and tail current analysis in astrocyte (A, C, E) and oligodendro-cyte precursor cells (B, D, F). **A, B:** Membrane currents were recorded in response to voltage steps. **C, D:** The tail current analysis in precursor cells. **E, F:** Currents (I) were measured 5 ms after the onset of the de- and hyperpolarizing pulses (dashed lines) and plotted as a function of the membrane potential (V_m). For further explanation, see legend to Figure 1.

were characterized by same types of voltage-activated K^+ channels as astrocyte precursors, but lacked voltage-activated Na^+ currents (Fig. 2B). In astrocytes and oligodendrocytes, the time constants of the outward and inward currents during and after the de- and hyperpolariz-ing pulses were independent of the amplitude of the pulse (Fig. 3A).

Tail Current Analysis

Tail currents were analyzed from measurements performed during a series of 20-ms test pulses from -130 mV to $+20$ mV following a depolarizing voltage step of 90 mV, i.e., by changing the holding potential from -70 mV to $+20$ mV, for 20 ms (Figs. 1C, D; 2C, D). The reversal potential (V_{rev}) of I_{tail} was determined from the current/voltage (I/V) relationship measured 5 ms after the onset of the test de- and hyperpolarizing pulses. V_{rev} of I_{tail} was shifted to more positive values in oligodendro-cytes than in astrocytes (Fig. 1E, F) or in glial precursor cells (Fig. 2E, F), even when comparable outward currents were evoked. V_{rev} of I_{tail} was -31.7 ± 2.58 mV (mean $\pm$ S.E.M., n = 53) in oligodendrocytes; $-57.9 \pm$

2.43 mV (n = 21) in astrocytes; -41.2 ± 3.44 mV (n = 36) in oligodendrocyte precursors; and $-52.1 \pm$ 1.32 mV (n = 43) in astrocyte precursors. There were no significant changes in the V_{rev} of I_{tail} during postnatal development from P5 to P11 (Fig. 3B).

Effect of amplitude of de- and hyperpolarizing prepulse. In all glial cell types V_{rev} of I_{tail} was depen-dent on the amplitude of the de- or hyperpolarizing prepulse (Fig. 4). When the voltage of the 20-ms prepulse changed from -60 to $+20$ mV, the V_{rev} of I_{tail} shifted to significantly more positive values in oligodendrocytes than in astrocytes and glial precursor cells (Fig. 4C). Similar results were observed when a series of hyperpolar-izing prepulses was used, i.e., when the voltage of the prepulse changed from -80 to -160 mV. In oligodendro-cytes, V_{rev} of I_{tail} shifted from -109.56 ± 5.14 mV (n = 5) after a -160-mV prepulse to -27.44 ± 4.78 mV (n = 5) after a $+20$-mV prepulse; while in astrocytes, V_{rev} of I_{tail} shifted from -94.64 ± 1.33 mV (n = 5) to -61.56 ± 3.86 mV (n = 5); in astrocyte precursors from -98.30 ± 6.02 mV (n = 5) to -57.11 ± 4.43 mV (n = 5); and in oligodendrocyte precursors from
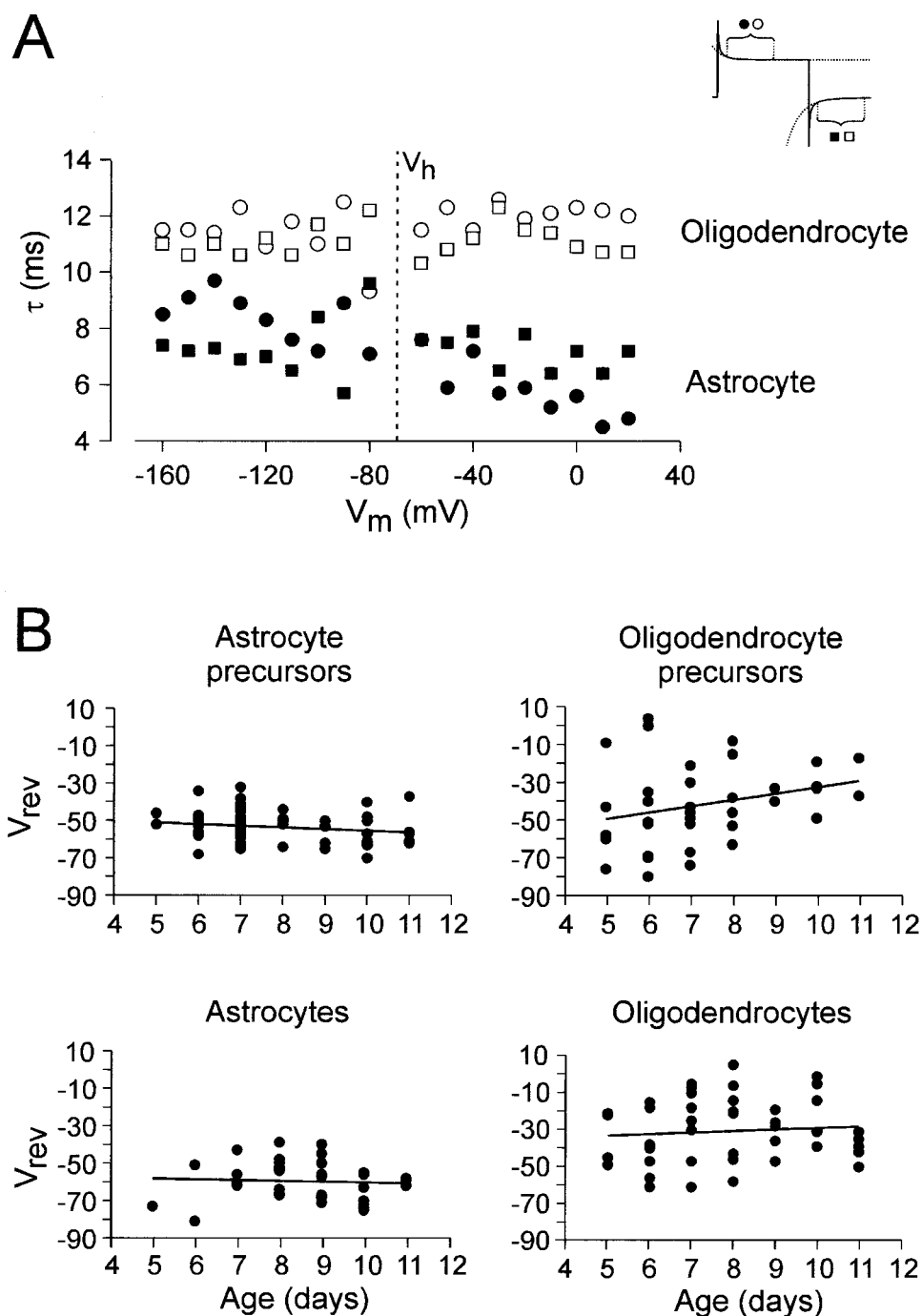
Fig. 3. Time constant of the membrane currents (A) and reversal potential of the tail currents during postnatal development (B). **A:** Time constant of the membrane currents evoked by the depolarizing and hyperpolarizing test pulses. Time constants (τ) of the membrane currents as a function of the voltage of the de- and hyperpolarizing pulse (V_m) are shown for an astrocyte (filled symbols) and an oligodendrocyte (open symbols). Values of the time constants were revealed by fitting the current traces monoexponentially during the interval of 5–30 ms after the onset (circles) or offset (squares) of the test pulses (indicated in the **inset**). **B:** Reversal potential of the tail currents in astrocytes, oligodendrocytes, and their precursor cells in the spinal cord gray matter during postnatal development. The values of reversal potential (V_{rev}) as a function of animal age and the corresponding linear regressions are shown for astrocytes, oligodendrocytes, astrocyte precursor and oligodendrocyte precursor cells. Slopes of the linear regression were not significantly different from zero, and the P values were 0.19 in astrocyte precursors, 0.09 in oligodendrocyte precursors, 0.73 in astrocytes, and 0.56 in oligodendrocytes (for details, see Materials and Methods).
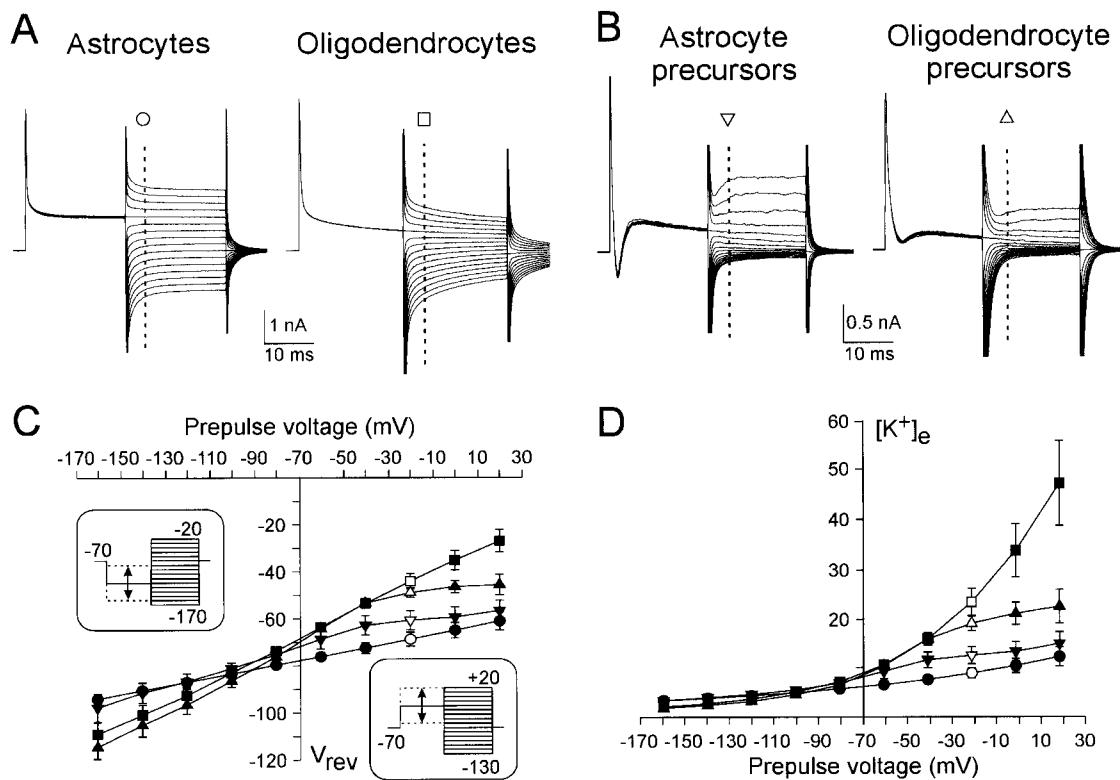
Fig. 4. Analysis of tail currents in astrocytes, oligodendrocytes, and their precursors after prepulses with different amplitudes. **A, B:** Astrocytes (circles), oligodendrocytes (squares), astrocyte precursors (inverted triangles), and oligodendrocyte precursors (triangles) were clamped from a holding potential of -70 mV to hyperpolarizing (-80 mV, -100 mV, -120 mV, -140 mV, and -160 mV) and depolarizing (-60 mV, -40 mV, -20 mV, 0 mV, and $+20$ mV) prepulses for 20 ms. After this prepulse, the membrane was clamped for 20 ms to increasing de- and hyperpolarizing potentials (pattern of voltage commands is shown in **insets**) ranging from -100 to $+30$ mV, with 10-mV increments. **C:** From traces obtained using the hyper- or depolarizing prepulses, currents (I) were measured 5 ms after the offset of the prepulse (dashed line) and the reversal potential (V_{rev}) of these currents were estimated. V_{rev} of tail currents in recordings with hyper- and depolarizing prepulses are plotted in the graph as a function of the prepulse voltage. Open symbol indicates the estimated value of V_{rev} using a depolarizing prepulse with a voltage of -20 mV, as shown in A and B. **D:** Values of V_{rev}, shown in C, were analyzed using the Nernst equation to yield the values of $[K^+]_e$, which were plotted for astrocytes and oligodendrocytes and their precursors as a function of the prepulse voltage.

-115.12 ± 7.11 mV (n = 5) to -46.13 ± 4.34 mV (n = 5). The glial membrane is almost selectively permeable for K^+; therefore, the membrane potential of the cell and the reversal potential for the K^+ current is given by the Nernst equation $V_{rev} = (RT/F) \ln ([K^+]_e/[K^+]_i)$ (Kuffler et al., 1966; see also Berger et al., 1991; Chvátal et al., 1997). The values of V_{rev} were thus recalculated to yield corresponding extracellular K^+ concentrations ($[K^+]_e$) according to the Nernst equation (Fig. 4D). In oligodendrocytes, a $+20$-mV prepulse evoked a significantly higher $[K^+]_e$ (47.04 ± 8.58 mM, n = 5) than in astrocytes (11.94 ± 1.95 mM, n = 5), astrocyte precursors (14.59 ± 2.41 mM, n = 5), or oligodendrocyte precursors (22.11 ± 3.43 mM, n = 5).

The values of V_{rev} of I_{tail} in glial precursor cells were affected by the activation of the delayed outwardly

rectifying and A-type K^+ currents during depolarizing prepulses, and therefore, further analysis was carried out only on astrocytes and oligodendrocytes.

Effect of prepulse duration.   In astrocytes and in oligodendrocytes, V_{rev} of I_{tail} was dependent on the duration of the de- or hyperpolarizing prepulse ranging from 3 to 50 ms (Fig. 5A). V_{rev} of I_{tail}, after a 50-ms depolarizing prepulse to $+20$ mV, was more positive in oligodendrocytes (-18.52 ± 1.95 mV, n = 5) than in astrocytes (-55.90 ± 4.40 mV, n = 5). Values of $[K^+]_e$ calculated from the values of V_{rev} of I_{tail} after a 50-ms prepulse were larger in oligodendrocytes (65.74 ± 10.28 mM, n = 5) than in astrocytes (15.12 ± 2.68 mM, n = 5; Fig. 5B).

Time course of tail currents. V_{rev} of I_{tail} was studied at different times, i.e., 5–50 ms, after the offset of
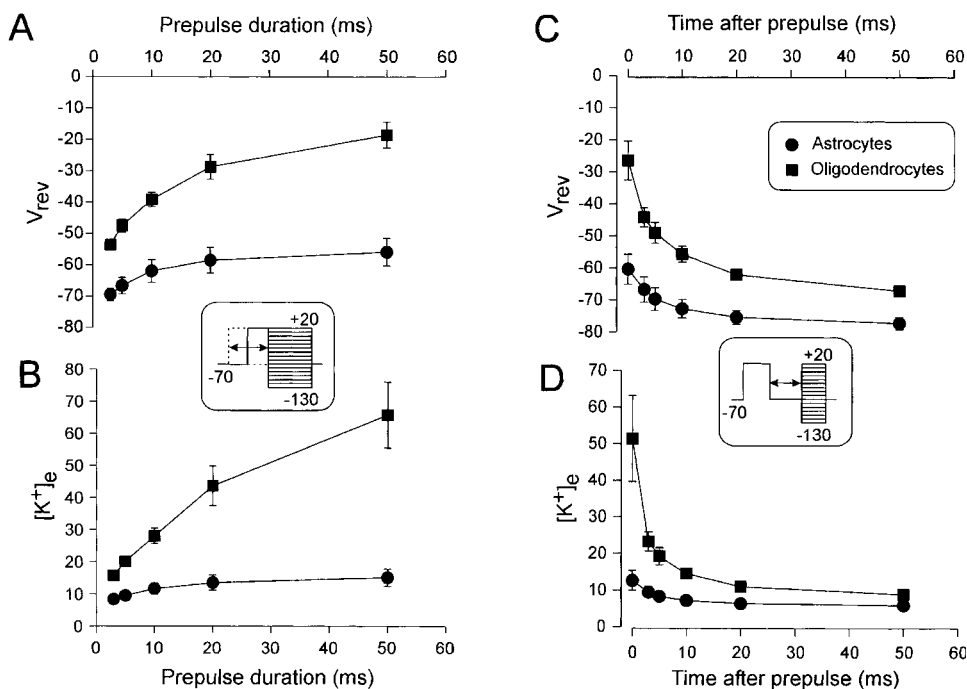
Fig. 5. Analysis of tail currents in astrocytes and oligodendrocytes after prepulses with variable time duration (A, B) and at variable times after the offset of the prepulse (C, D). **A, B:** The reversal potentials (V_{rev}) of tail currents in astrocytes (circles) and oligodendrocytes (squares) in recordings with 3 ms, 5 ms, 10 ms, 20 ms, and 50 ms prepulses (A) and values of $[K^+]_e$ (B) are plotted in the graphs as a function of the prepulse duration (indicated by the arrows in the **inset**). For further details, see legend to Figure 4. **C, D:** The reversal potentials (V_{rev}) in recordings 0 ms, 3 ms, 5 ms, 10 ms, 20 ms, and 50 ms after the offset of the depolarizing prepulse (C) and values of $[K^+]_e$ (D) are plotted in the graphs as a function of the prepulse duration (indicated by the arrows in the **inset**). For further details, see legend to Figure 4.

the depolarizing prepulse (Fig. 5C). The resulting time course of V_{rev} of I_{tail} measured in astrocytes and oligodendrocytes revealed that even though the depolarizing prepulse evoked larger I_{tail} in oligodendrocytes than in astrocytes, the half-decay time of V_{rev} of I_{tail} was 4 ms in both types of cells. Similarly, the half-decay time of $[K^+]_e$ calculated from the values of V_{rev} was 3 ms in both astrocytes and oligodendrocytes and thus did not reveal differences in the time course of the redistribution of K^+ (Fig. 5D).

Effect of Cell Swelling Induced by the Application of 50 mM K⁺ and Hypotonic Solution

Studies carried out in cell cultures revealed that application of high K^+ in the ACF produces glial cell swelling (Walz and Mukerji, 1988; Walz, 1992; Kimelberg et al., 1995). Recently, studies performed in vivo also showed that ECS shrinks due to cell swelling (Svoboda and Syková, 1991; Voříšek and Syková, 1997). Therefore, we studied the effect of 50 mM K^+ and hypotonic ACF (200 mmol/kg) on the resting membrane potential (V_m) and K^+ accumulation around astrocytes

and oligodendrocytes produced by the depolarizing prepulses, as calculated from the V_{rev} of I_{tail}, (Figs. 6, 7).

V_m of astrocytes and oligodendrocytes was measured for each I_{tail} recording by switching the EPC-9 amplifier to the current clamp mode before and during the 20 min application of 50 mM K^+ in the ACF. Under control conditions, i.e., during perfusion with 3 mM K^+ in the ACF, V_m of astrocytes and oligodendrocytes was -75.74 ± 1.9 mV (n = 5) and -62.07 ± 4.3 mV (n = 5), respectively. Thus, V_m was shifted to more positive values than the values of the theoretical K^+ equilibrium potential $V_m = -95.21$ mV, as predicted from the Nernst equation (Fig. 6A, dashed column). During the increase of $[K^+]_e$ to 50 mM, V_m of astrocytes and oligodendrocytes shifted to -19.18 ± 1.1 mV (n = 5) and -18.9 ± 0.9 mV (n = 4), respectively (Fig. 6A, C). The measured values of V_m followed the theoretical K^+ equilibrium potential of -24.14 mV. The Nernst equation was also used to calculate $[K^+]_e$ from the values of V_m. In astrocytes, $[K^+]_e$ increased from 6.6 ± 0.5 to 61.04 ± 2.4 mM and in oligodendrocytes from 11.62 ± 1.8 to 61.76 ± 2.3 mM (Fig. 6B, D).
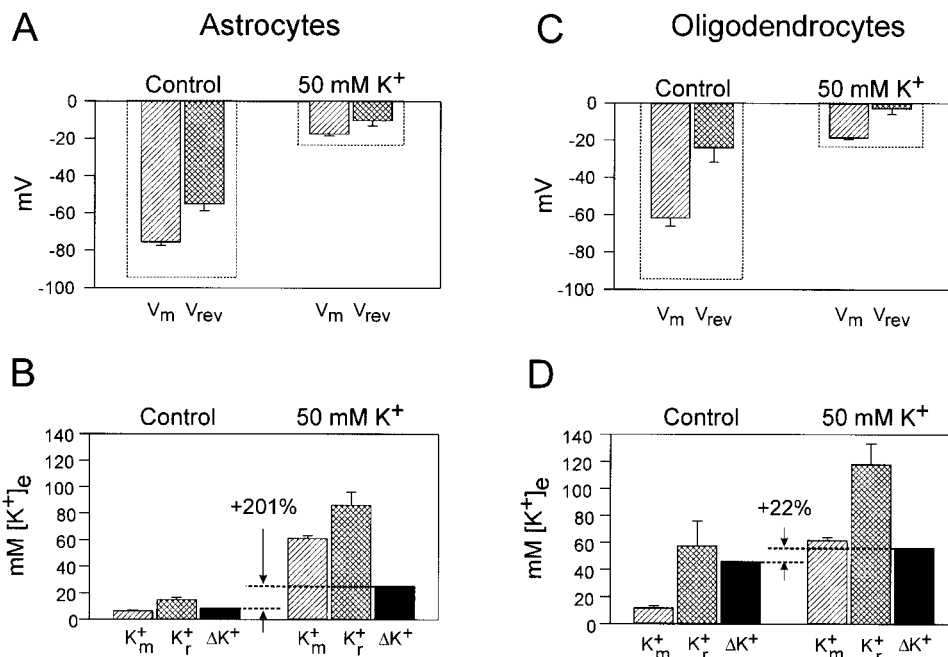
Fig. 6. Effect of 50 mM K$^+$ on the membrane potential and reversal potential of tail currents in astrocytes and oligodendrocytes. **A, C:** Values of membrane potentials (V$_m$) and reversal potentials of the tail currents (V$_{rev}$) in astrocytes and oligodendrocytes prior to and during the application of 50 mM K$^+$ in the artificial cerebrospinal fluid (ACF). Dashed columns indicate the theoretical values as calculated from the Nernst equation. **B, D:** Using the Nernst equation, [K$^+$]$_e$ was calculated from the mean values of V$_m$ (K$_m^+$) and V$_{rev}$ (K$_r^+$) and their difference (ΔK$^+$).

V$_{rev}$ of I$_{tail}$ was measured from the recordings described in the legend to Figure 1C and D, i.e., by applying a depolarizing prepulse with the series of concomitant de- and hyperpolarizing pulses before and during the application of 50 mM K$^+$ in the ACF. Under control conditions, a depolarizing prepulse produced a larger accumulation of K$^+$ around oligodendrocytes than around astrocytes and thus, the resting level of V$_{rev}$ of I$_{tail}$ in oligodendrocytes shifted to more positive values than in astrocytes (Fig. 6A, C). The application of 50 mM K$^+$ evoked a larger increase in V$_{rev}$ of I$_{tail}$ in astrocytes (from -55.40 ± 3.2 to -10.96 ± 2.8 mV, n = 5) than in oligodendrocytes (from -24.27 ± 7.7 to 3.09 ± 3.1 mV, n = 4). [K$^+$]$_e$ calculated from the mean values of V$_{rev}$ of I$_{tail}$ increased from 14.95 ± 1.7 mM to 86.33 ± 9.7 mM in astrocytes and from 57.51 ± 18.4 mM to 117.83 ± 15.5 mM in oligodendrocytes (Fig. 6B, D).

We calculated the net increase in [K$^+$]$_e$ evoked by depolarizing prepulses before and during the application of 50 mM K$^+$ by subtracting the values of [K$^+$]$_e$ calculated from the mean values of V$_{rev}$ of I$_{tail}$ from the values of [K$^+$]$_e$ calculated from the values of V$_m$ (Fig. 6B, D, black bars), in order to follow the effect of the K$^+$-induced cell swelling on the K$^+$ accumulation in the ECS. In astrocytes, the net increase in [K$^+$]$_e$ was only 8.4 mM before the application of 50 mM K$^+$, while during

the application of 50 mM K$^+$, it rose to 25.3 mM. Thus, the application of 50 mM K$^+$ evoked an increase in [K$^+$]$_e$, produced by depolarizing prepulses, of about 201% (Fig. 6B). In oligodendrocytes, such an increase was not found. Prior to and during the application of 50 mM K$^+$, the differences in [K$^+$]$_e$ were 45.95 mM and 56.1 mM, respectively, and thus the increase was about 22% (Fig. 6D).

To test whether the observed changes arise from ECS shrinkage induced by cell swelling, we also studied V$_m$ and V$_{rev}$ of I$_{tail}$ in hypotonic ACF, by changing the osmolality of ACF from 300 mmol/kg to 200 mmol/kg (Fig. 7). Hypotonic ACF did not significantly affect V$_m$ in either astrocytes or oligodendrocytes. On the other hand, it had a marked effect on the V$_{rev}$ of I$_{tail}$ in astrocytes but not in oligodendrocytes (Fig. 7A, C). In astrocytes, V$_{rev}$ of I$_{tail}$ increased from -52.10 ± 1.34 (n = 4) in normal, to -31.60 ± 6.84 in hypotonic ACF. [K$^+$]$_e$ calculated from the mean values of V$_{rev}$ of I$_{tail}$ using the Nernst equation increased from 16.59 ± 0.87 mM to 41.91 ± 12.6 mM (Fig. 7B). The net increase in [K$^+$]$_e$ evoked by depolarizing pulses rose from 10.7 mM in normal to 36.3 mM in hypotonic ACF, i.e., by 239% (Fig. 7B, black bars). In oligodendrocytes, the net increase in [K$^+$]$_e$ evoked by depolarizing pulses was much smaller, from 36.7 mM in
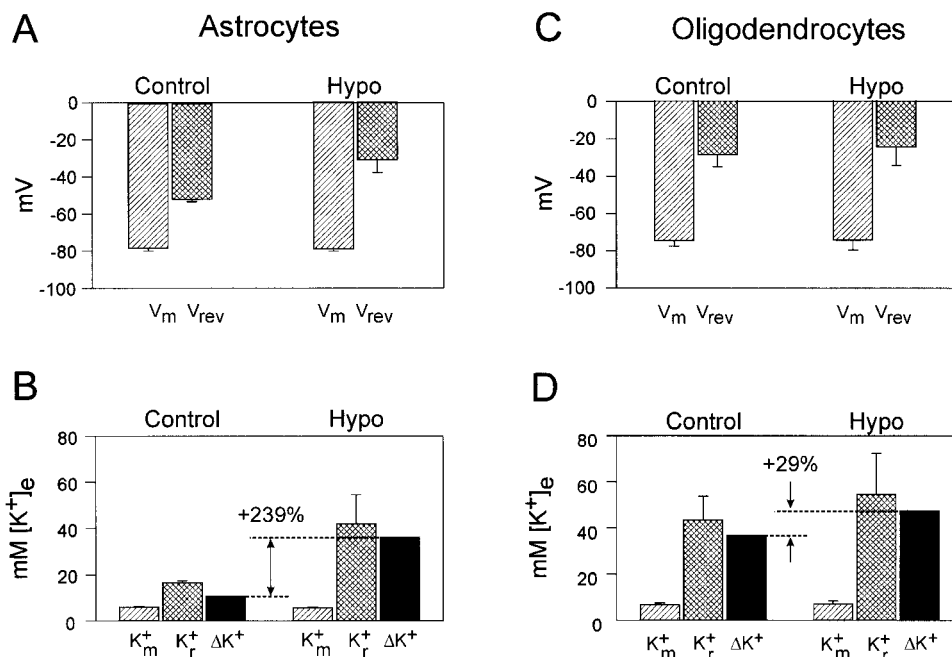
Fig. 7. Effect of hypotonic artificial cerebrospinal fluid (ACF) on the membrane potential and reversal potential of tail currents in astrocytes and oligodendrocytes. **A, C:** Values of membrane potentials (V$_m$) and reversal potentials of the tail currents (V$_{rev}$) prior to and during the application of hypotonic ACF. **B, D:** Using the Nernst equation, [K$^+$]$_e$ was calculated from the mean values of V$_m$ (K$_m^+$) and V$_{rev}$ (K$_r^+$) and their difference (ΔK$^+$).

normal to 47.5 mM in hypotonic ACF, i.e., by 29% (Fig. 7D, black bars).

DISCUSSION

Tail Currents Arise From the Rapid Transmembrane Shift of K$^+$

In the present study performed on spinal cord slices, we have found that exclusively oligodendrocytes were characterized by passive but decaying K$^+$ currents with prominent tail currents after the offset of the de- or hyperpolarizing prepulse. Our present results, as well as studies performed on spinal cord white matter (Chvátal, Anděrová and Syková, unpublished results), are in agreement with studies performed on mice and rat brain slices in which oligodendrocytes were studied in the white matter (corpus callosum) and de- or hyperpolarizing voltage jumps induced prominent tail currents (Berger et al., 1991; Chvátal et al., 1997).

In contrast, electrophysiological investigations of oligodendrocytes in culture did not reveal the presence of tail currents (Sontheimer and Kettenmann, 1988; Sontheimer et al., 1989). In an attempt to reconcile these findings, Berger et al. (1991) suggested that the current decay observed in oligodendrocytes in brain slices of the corpus callosum is produced by a shift in the K$^+$ gradient across

the glial membrane. Their suggestion was based on the following observations: first, depolarizing or hyperpolarizing voltage jumps produce a more positive or a more negative shift of V$_{rev}$ of I$_{tail}$, respectively. This behavior is compatible with an outward movement of K$^+$ during depolarization and an inward movement during hyperpolarization. Second, the time decay during, as well as after, the voltage jump is independent of voltage, but varies markedly from cell to cell. This finding is in agreement with our present experiments performed on oligodendrocytes in the gray matter of spinal cord slices. Furthermore, the glial membrane potential is strongly dependent on [K$^+$]$_e$. In our previous study, the superfusion of rat spinal cord slices with 55 mM K$^+$ shifted the reversal potential of all glial cell types, including oligodendrocytes, to -16 mV, which is close to the estimated equilibrium potential of -23 mV (Chvátal et al., 1995). Single-channel patch-clamp studies of oligodendrocytes in culture revealed the presence of K$^+$ channels, which were affected by changes in extracellular K$^+$ (Kettenmann et al., 1982, 1984). The I/V curve of K$^+$ channels shifted as predicted by the Nernst equation for an exclusive K$^+$ conductance. These highly selective K$^+$ channels were the only type of channels which were found in the membrane of cultured oligodendrocytes (see also Kettenmann, 1986). Finally, it was shown in experi-

ments performed in mouse corpus callosum as well as in rat spinal cord gray matter, that the application of Ba^{2+}, a K^+ channel blocker, inhibited tail currents after de- and hyperpolarizing voltage steps (Berger et al., 1991; Chvátal et al., 1995).

The resting membrane potential of astrocytes and oligodendrocytes observed in our experiments was more positive than predicted, probably due to the fact that the membrane of glial cells under resting conditions is also permeable for other ions (Ballanyi et al., 1987; Lascola et al., 1996, 1998), thus possibly explaining the observed discrepancies. Our calculations were based on the prediction that the glial membrane is permeable only for K^+. We did not consider potassium gradients inside the cells or changes in intracellular $[K^+]$, which also may take place in both types of glial cells even when the intracellular composition is controlled by the patch pipette (Kettenmann et al., 1983). However, neither the presumed permeability of the glial membrane for other ions, nor potassium gradients or changes in intracellular $[K^+]$, can explain our findings, in which a prominent shift of V_{rev} of I_{tail} to more positive values was observed in oligodendrocytes but not in astrocytes or glial precursor cells, even when comparable outward currents were evoked (see also Chvátal et al., 1997).

We may therefore conclude that the tail currents observed in oligodendrocytes, in gray as well as in white matter, represent a rapid shift of K^+ caused by a change in the K^+ gradient across the cell membrane during the voltage step. It is evident that such a rapid shift of K^+ is mediated through K^+ channels or by K^+/Cl^- uptake (Kettenmann, 1987) but not by Na^+/K^+ ATPase activity. The time course of the tail currents is in the range of milliseconds, while the uptake of K^+ mediated via the activity of Na^+/K^+ ATPase may last several minutes (Kettenmann et al., 1987) and, in addition, requires an increased intracellular Na^+ concentration (Tang et al., 1980).

Why Do Only Oligodendrocytes Have Prominent Tail Currents?

In the study of Berger et al. (1991) performed on mouse white matter, where the majority of cells of the oligodendrocyte lineage is found, prominent tail currents were observed in mature oligodendrocytes. No or very small tail currents were observed in oligodendrocyte precursor cells. Since the tail currents are produced by a shift in the K^+ gradient, the authors suggested that K^+ is extruded into the extracellular space, which is more "compacted" around oligodendrocytes than around oligodendrocyte precursors (Berger et al., 1991). It was shown in the study of Chvátal et al. (1997) that the appearance of K^+ tail currents in glial cells of the oligodendrocyte

lineage coincides with the decrease in the extracellular space in white matter during postnatal development.

Values of oligodendrocyte I_{tail} recorded in our experiments in spinal cord gray matter were in the same range as in the white matter (corpus callosum) of the rat (Chvátal et al., 1997). Assuming that the V_{rev} of I_{tail} is determined by the K^+ gradient across the glial membrane, depolarizing pulses evoke a significantly larger increase in $[K^+]_e$ around oligodendrocytes than around astrocytes and glial precursor cells. Our findings with changed depolarizing prepulse duration and amplitude, as well as the rapid recovery of $[K^+]_e$ after the offset of the depolarizing voltage jump, also correlate with the rapid K^+ movement across the glial membrane.

In mouse and rat corpus callosum, oligodendrocyte precursors at P10 expressed significantly smaller tail currents than oligodendrocytes at P20 (Berger et al., 1991; Chvátal et al., 1997). The above studies raised the question whether the appearance and increase of tail currents in oligodendrocytes develop concomitantly with the "maturation" of the nervous tissue, i.e., the outgrowth and prolongation of cell processes and changes in the extracellular matrix composition, or whether the presence of large tail currents is independent of the changes in ECS volume during postnatal development. It was shown by Prokopová et al. (1997) that the extracellular volume fraction, measured over a volume on the order of 10^{-3} mm^3, significantly decreases in spinal cord gray matter during postnatal development between P4 and P8. However, we did not observe significant changes of V_{rev} of I_{tail} within each glial cell type during the period from P5 to P11. This may be explained by the fact that the values of V_{rev} of I_{tail} represent changes in $[K^+]_e$ not in the bulk of the tissue but in the immediate vicinity of the glial membrane. The appearance of tail currents in oligodendrocytes is therefore not related to the average ECS volume fraction of the tissue, but at the cellular level, the ECS could be more "compact" in the close vicinity of oligodendrocytes. An increasing number of oligodendrocytes surrounded by a "compact" ECS might be, together with the elongation and branching of astrocyte processes (Takahashi et al., 1990) and axonal and dendritic outgrowth (Bicknell and Beal, 1984), an additional factor responsible for the decrease in the ECS volume during postnatal development (Fig. 8A).

In astrocytes, the application of 50 mM K^+ or hypotonic ACF produced a prominent increase in $[K^+]_e$ evoked by the depolarizing prepulse. Such an increase was not observed in oligodendrocytes. Since the amplitude of the depolarizing prepulses and the intracellular concentration of K^+ remained unchanged, a possible explanation for this finding could be the shrinkage of the ECS volume around astrocytes during the application of 50 mM K^+. Swelling of astrocytes in ACF containing
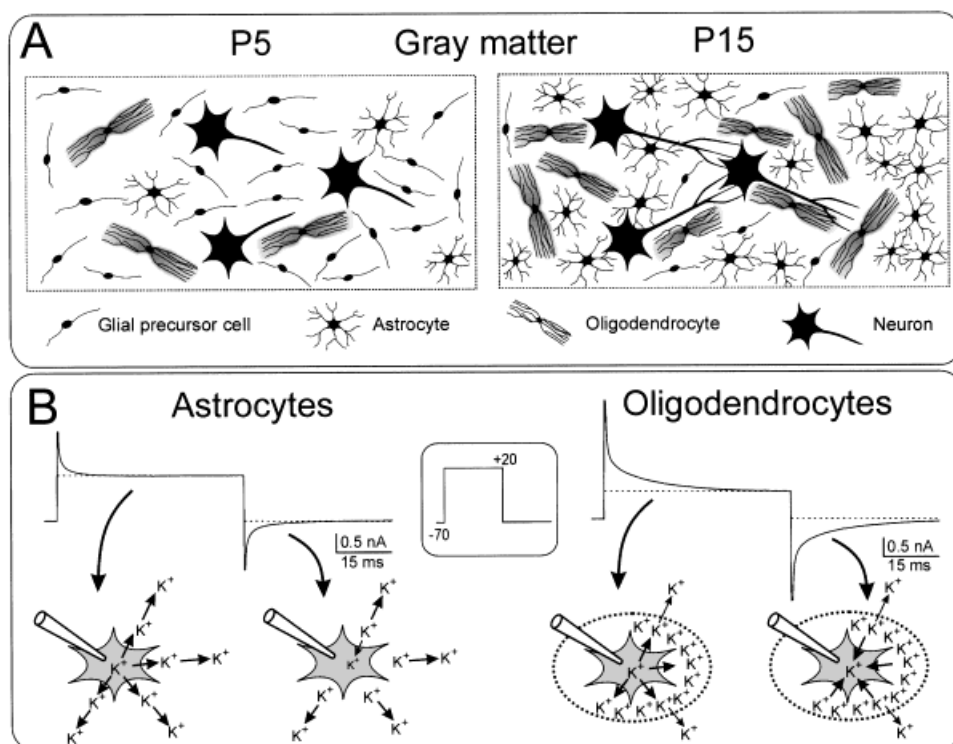
Fig. 8. Hypotheses of the developmental changes in the spinal cord gray matter (A) and the K$^+$ movements across astrocytic and oligodendrocytic membrane (B). **A:** Drawing of the developmental changes in the spinal cord gray matter between postnatal day (P) 5 and P15. At P5, the majority of the cells are glial precursors and the ECS volume remains relatively large. At P15, there is a substantial increase in the number of mature astrocytes and oligodendrocytes together with the elongation and branching of glial processes, axonal and dendritic outgrowth and a decrease of the ECS volume. The gray shading between oligodendrocyte processes indicates the "compact" ECS in the vicinity of the oligodendrocyte membrane. **B:** Hypothesis of the K$^+$ shift across astrocytic and oligodendrocytic membranes during and after the depolarizing pulse on a cellular level. In astrocytes, a small amount of K$^+$ reenters the cell after the offset of the voltage command, creating a very small tail current. In oligodendrocytes, K$^+$ accumulates in the vicinity of the cell membrane due to presumed diffusion barriers (dashed ellipse) and thus produces prominent tail currents after the offset of the voltage command. For further explanation, see text.

high K$^+$ and reciprocally reduced Na$^+$ or in hypotonic ACF has been described in many tissue culture studies (Moller et al., 1974; Walz et Mukerji, 1988; Petito et al., 1991; Walz, 1992; Kimelberg et al., 1995). Our hypothesis is also supported by the recent study of Syková et al. (1999), in which the application of 50 mM K$^+$ evoked in the dorsal horn gray matter of the isolated rat spinal cord a dramatic decrease in the average ESC volume fraction from 0.23 to 0.07, i.e., by 70%, due to glial swelling. Thus in astrocytes, the dynamic decrease in the ECS volume evoked a shift of the V$_{rev}$ of I$_{tail}$ to more positive values, as a result of the increased K$^+$ accumulation around the cell membrane. In oligodendrocytes, surrounded by a "compact" ECS, a further decrease in the ECS volume did not evoke such an effect, indicating that this type of glial cell most likely does not contribute to the decrease in the ECS volume.

Our results clearly show that the oligodendrocyte is the only cell type in spinal cord gray matter that expresses prominent tail currents. We suggest that the larger tail currents might result from a more "compact" extracellular space around oligodendrocytes and that this property is unique to oligodendrocytes in white as well as in gray matter. Since the observed properties of glial potassium tail currents were found in spinal cord slices, the question remains whether effect of ECS volume changes on E$_{rev}$ of I$_{tail}$ also occurs in the brain in vivo. It was shown by Moller et al. (1974), using the [^{14}C]inulin uptake method with concomitant fixation technique, that brain slices show an altered fluid distribution as a result of an in vitro incubation. It therefore cannot be excluded that the differences between astrocytes and oligodendrocytes may apply only in brain slices but not in the brain in vivo. On the other hand, experiments performed by means of the

real-time iontophoretic method in unfixed tissue did not show any substantial differences in the ECS volume fraction and other diffusion parameters between brain slices and the brain in vivo (for reviews, see Syková, 1997; Nicholson and Syková, 1998).

Role of Oligodendrocyte Tail Currents in K+ Clearance

In contrast to the well-known property of oligodendrocytes in white matter to produce and maintain myelin sheaths and their proposed ability to buffer K^+ changes in the ECS (Orkand, 1986; for reviews see Walz, 1989; Barres, 1991; Szuchet, 1995), the function of oligodendrocytes in gray matter, also called ''perivascular,'' is not clear (Miller et al., 1994).

Our results indicate that oligodendrocytes might play an important role in the K^+ buffering. In addition to the models of K^+ dynamics in nervous tissue described previously (Nicholson, 1980; Gardner-Medwin, 1983; Orkand, 1986; Amédée et al., 1997), we propose a model that explains the differences in the K^+ shift across astrocytic and oligodendrocytic membranes on a cellular level. Our model is based on the assumption that during the depolarizing pulse, K^+ is extruded from the cell to the extracellular space (Fig. 8B). In astrocytes, extruded K^+ freely moves away from the membrane, so within several milliseconds a steady-state is established, i.e., the majority of K^+ that is leaving the cell is freely redistributed in the ECS. After the offset of the voltage command, only a small amount of K^+ reenters the cell, creating a very small tail current. In oligodendrocytes, presumed diffusion barriers (Fig. 8B, dashed ellipse) prevent K^+ from moving freely away, and thus K^+ accumulates in the vicinity of the cell membrane. During this accumulation, a new K^+ equilibrium is established, which is reflected by the decreasing current during the voltage step. After the offset of the depolarizing prepulse, K^+ moves back to the cell and produces prominent tail currents. The time course of K^+ shifts is in the range of milliseconds, and thus they are not mediated by ATP-based uptake mechanisms.

The question remains, what are the diffusion barriers that slow down the movement of K^+ away from the oligodendrocyte membrane? The presence of tail currents in oligodendrocytes in brain slices, but not in tissue culture with an infinite ECS volume (Sontheimer and Kettenmann, 1988; Sontheimer et al., 1989), indicates that the diffusion barriers are present only in the compacted nervous tissue. One of the possible mechanisms of the more effective removal of K^+ away from the astrocytic membrane might be the spatial K^+ buffering performed by the network of astrocytes connected via gap junctions (Hounsgaard and Nicholson, 1983). However, our experiments with 50 mM K^+ and hypotonic ACF indicate that the larger accumulation of K^+ around oligodendrocytes is most likely caused by a smaller ECS in the vicinity of this type of cell. In addition, we cannot entirely exclude possible differences in the molecules of the extracellular matrix around astrocytes and oligodendrocytes, e.g., the region-dependent distribution pattern of perineuronal nets, which represent extracellular accumulations of matrix proteoglycans, and its association with certain types of neurons (Brückner et al., 1996). The unique electrophysiological behavior of oligodendrocytes could also be correlated with their specific morphology, i.e., long and parallel processes, not seen in other types of glial cells, which corresponds to their tight contact with axons.

Our data show that depolarization of glial cells in the spinal cord gray matter evokes a more substantial increase in extracellular K^+ concentration around oligodendrocytes than around astrocytes. Since the major source of K^+ during neuronal activity is neurons, the relative distribution of each type of glial cell to K^+ homeostasis in the CNS is not yet clearly defined. There is no doubt that the major role in K^+ homeostasis is carried out by astrocytes, either by K^+ uptake or by a K^+ spatial buffer mechanism (see also Hertz et al., 1990). However, electrophysiological properties of oligodendrocytes, i.e., the K^+ influx indicated by the presence of tail currents, indicates that this type of cell may also contribute to the regulation of K^+ changes arising from neuronal activity.

REFERENCES

Amédée T, Robert A, Coles JA. 1997. Potassium homeostasis and glial energy metabolism. Glia 21:46–55.

Ballanyi K, Grafe P, Ten Bruggencate G. 1987. Ion activities and potassium uptake mechanisms of glial cells in guinea-pig olfactory cortex slices. J Physiol (Lond) 382:159–174.

Barres BA. 1991. New roles for glia. J Neurosci 11:3685-3694.

Barres BA, Chun LLY, Corey DP. 1990. Ion channels in vertebrate glia. Annu Rev Neurosci 13:441–474.

Berger T, Schnitzer J, Kettenmann H. 1991. Developmental changes in the membrane current pattern, K^+ buffer capacity and morphology of glial cells in the corpus callosum slice. J Neurosci 11:3008–3024.

Bicknell HR, Beal JA. 1984. Axonal and dendritic development of substantia gelatinosa neurons in the lumbosacral spinal cord of the rat. J Comp Neurol 226:508–522.

Brückner G, Bringmann A, Köppe G, Härtig W, Brauer K. 1996. In vivo and in vitro labelling of perineuronal nets in rat brain. Brain Res 720:84–92.

Chvátal A, Pastor A, Mauch M, Syková E, Kettenmann H. 1995. Distinct populations of identified glial cells in the developing rat spinal cord: Ion channel properties and cell morphology. Eur J Neurosci 7:129–142.

Chvátal A, Berger T, Voříšek I, Orkand RK, Kettenmann H, Syková E. 1997. Changes in glial K^+ currents with decreased extracellular volume in developing rat white matter. J Neurosci Res 49:98–106.

Duffy S, Fraser DD, MacVicar BA. 1995. Potassium channels. In: Kettenmann H, Ransom BR, editors. Neuroglia. New York: Oxford University Press. p. 185–201.

Edwards FA, Konnerth A, Sakmann B, Takahashi T. 1989. A thin slice preparation for patch clamp recordings from neurones of the mammalian central nervous system. Pflügers Arch 414:600–612.

Gardner-Medwin AR. 1983. A study of the mechanisms by which potassium moves through brain tissue in the rat. J Physiol (Lond) 335:353–374.

Hamill OP, Marty A, Neher E, Sakmann B, Sigworth FJ. 1981. Improved patch-clamp techniques for high-resolution current recording from cells and cell-free membrane patches. Pflügers Arch 391:85–100.

Hertz L, Soliven B, Hertz E, Szuchet S, Nelson DJ. 1990. Channel-mediated and carrier-mediated uptake of K⁺ into cultured ovine oligodendrocytes. Glia 3:550–557.

Hounsgaard J, Nicholson C. 1983. Potassium accumulation around individual Purkinje cells in cerebellar slices from the guinea-pig. J Physiol (Lond) 340:359–388.

Kettenmann H. 1986. Oligodendrocytes control extracellular potassium by active uptake and spatial buffering. Adv Biosci 61:155–163.

Kettenmann H. 1987. K⁺ and Cl⁻ uptake by cultured oligodendrocytes. Can J Physiol Pharmacol 65:1033–1037.

Kettenmann H, Orkand RK, Lux HD, Schachner M. 1982. Single potassium channel currents in cultured mouse oligodendrocytes. Neurosci Lett 32:41–46.

Kettenmann H, Sonnhof U, Schachner M. 1983. Exclusive potassium dependence of the membrane potential in cultured mouse oligodendrocytes. J Neurosci 3:500–505.

Kettenmann H, Orkand RK, Lux HD. 1984. Some properties of single potassium channels in cultured oligodendrocytes. Pflugers Arch 400:215–221.

Kettenmann H, Syková E, Orkand RK, Schachner M. 1987. Glial potassium uptake following depletion by intracellular ionophoresis. Pflügers Arch 410:1–6.

Kimelberg HK, Rutledge E, Goderie S, Charniga C. 1995. Astrocytic swelling due to hypotonic or high K⁺ medium causes inhibition of glutamate and aspartate uptake and increases their release. J Cereb Blood Flow Metab 15:409–416.

Kuffler SW, Nicholls JG, Orkand RK. 1966. Physiological properties of glial cells in the central nervous system of amphibia. J Neurophysiol 29:768–787.

Lascola CD, Kraig RP. 1996. Whole-cell chloride currents in rat astrocytes accompany changes in cell morphology. J Neurosci 16:2532–2545.

Lascola CD, Nelson DJ, Kraig RP. 1998. Cytoskeletal actin gates a Cl⁻ channel in neocortical astrocytes. J Neurosci 18:1679–1692.

Miller RH, Zhang H, Fok-Seang J. 1994. Glial cell heterogeneity in the mammalian spinal cord. Persp Dev Neurobiol 2:225–231.

Moller M, Mollgard K, Lund-Andersen H, Hertz L. 1974. Concordance between morphological and biochemical estimates of fluid spaces in rat brain cortex slices. Exp Brain Res 22:299–314.

Nicholson C. 1980. Dynamics of the brain cell microenvironment. Neurosci Res Progr Bull 18:177–322.

Nicholson C, Syková E. 1998. Extracellular space structure revealed by diffusion analysis. Trends Neurosci 21:207–215.

Orkand RK. 1986. Introductory remarks: glial-Interstitial fluid exchange. Ann NY Acad Sci 481:269–272.

Pastor A, Chvátal A, Syková E, Kettenmann H. 1995. Glycine- and GABA-activated currents in identified glial cells of the developing rat spinal cord slice. Eur J Neurosci 7:1188–1198.

Petito CK, Juurlink BHJ, Herz L. 1991. In vitro models differentiating between direct and indirect effects of ischemia on astrocytes. Exp Neurol 113:364–372.

Prokopová Š, Vargová L, Syková E. 1997. Heterogenous and anisotropic diffusion in the developing rat spinal cord. NeuroReport 8:3527–3532.

Sontheimer H, Kettenmann H. 1988. Heterogeneity of potassium currents in cultured oligodendrocytes. Glia 1:415–420.

Sontheimer H, Trotter J, Schachner M, Kettenmann H. 1989. Channel expression correlates with differentiation stage during the development of oligodendrocytes from their precursor cells in culture. Neuron 2:1135–1145.

Steinhäuser C, Berger T, Frotscher M, Kettenmann H. 1992. Heterogeneity in the membrane current pattern of identified glial cells in the hippocampal slice. Eur J Neurosci 4:472–484.

Svoboda J, Syková E. 1991. Extracellular space volume changes in the rat spinal cord produced by nerve stimulation and peripheral injury. Brain Res 560:216–224.

Syková E. 1983. Extracellular K⁺ accumulation in the central nervous system. Prog Biophys Molec Biol 42:135–189.

Syková E. 1992. Ionic and volume changes in the microenvironment of nerve and receptor cells. In: Ottoson D, series editor. Progress in sensory physiology 13. Heidelberg: Springer. p. 1–167.

Syková E. 1997. The extracellular space in the CNS: its regulation, volume and geometry in normal and pathological neuronal function. The Neuroscientist 3:28–41.

Syková E, Vargová L, Prokopová Š, Šimonová Z. 1999. Glial swelling and astrogliosis produce diffusion barriers in the rat spinal cord. Glia 25:56–70.

Szuchet S. 1995. The morphology and ultrastructure of oligodendrocytes and their functional implications. In: Kettenmann H, Ransom BR, editors. Neuroglia. New York: Oxford University Press. p. 23–43.

Takahashi T, Misson J-P, Caviness VS Jr. 1990. Glial process elongation and branching in the developing murine neocortex: a qualitative and quantitative immunohistochemical analysis. J Comp Neurol 302:15–28.

Tang C-M, Cohen MW, Orkand RK. 1980. Electrogenic pumps in axons and neuroglia and extracellular potassium homeostasis. Brain Res 194:283–286.

Voříšek I, Syková E. 1997. Ischemia-induced changes in the extracellular space diffusion parameters, K⁺, and pH in the developing rat cortex and corpus callosum. J Cereb Blood Flow Metab 17:191–203.

Walz W. 1989. Role of glial cells in the regulation of the brain ion microenvironment. Prog Neurobiol 33:309–333.

Walz W. 1992. Mechanism of rapid K⁺-induced swelling of mouse astrocytes. Neurosci Lett 135:243–246.

Walz W, Mukerji S. 1988. KCl movements during potassium-induced cytotoxic swelling of cultured astrocytes. Exp Neurol 99:17–29.

Žiak D, Chvátal A, Syková E. 1998. Glutamate-, kainate- and NMDA-evoked membrane currents in identified glial cells in rat spinal cord slice. Physiol Res 47:365–375.